

Elimination of the Disulfide Bridge in the Rieske Iron–Sulfur Protein Allows Assembly of the [2Fe-2S] Cluster into the Rieske Protein but Damages the Ubiquinol Oxidation Site in the Cytochrome *bc*₁ Complex[†]

Torsten Merbitz-Zahradnik,[‡] Klaus Zwicker,[§] Jürgen H. Nett,[‡] Thomas A. Link,^{||} and Bernard L. Trumpower^{*,‡}

Department of Biochemistry, Dartmouth Medical School, Hanover, New Hampshire 03755, Institut für Biochemie I-Molekulare Bioenergetik, Universitätsklinikum Frankfurt, ZBC, D-60590 Frankfurt, Germany, and Institut für Biophysik, Johann Wolfgang Goethe-Universität, D-60590 Frankfurt, Germany

Received July 29, 2003; Revised Manuscript Received September 25, 2003

ABSTRACT: The [2Fe-2S] cluster of the Rieske iron–sulfur protein is held between two loops of the protein that are connected by a disulfide bridge. We have replaced the two cysteines that form the disulfide bridge in the Rieske protein of *Saccharomyces cerevisiae* with tyrosine and leucine, and tyrosine and valine, to evaluate the effects of the disulfide bridge on assembly, stability, and thermodynamic properties of the Rieske iron–sulfur cluster. EPR spectra of the Rieske proteins lacking the disulfide bridge indicate the iron–sulfur cluster is assembled in the absence of the disulfide bridge, but there are significant shifts in all *g* values, indicating a change in the electronic structure of the [2Fe-2S] iron–sulfur center. In addition, the midpoint potential of the iron–sulfur cluster is lowered from 265 mV in the Rieske protein from wild-type yeast to 150 mV in the protein from the C164Y/C180L mutant and to 160 mV in the protein from the C164Y/C180V mutant. Ubiquinol-cytochrome *c* reductase activities of the *bc*₁ complexes with Rieske proteins lacking the disulfide bridge are less than 1% of the activity of the *bc*₁ complex from wild-type yeast, even though normal amounts of the iron–sulfur protein are present as judged by Western blot analysis. These activities are lower than the 105–115 mV decrease in the midpoint potential of the Rieske iron–sulfur cluster can account for. Pre-steady-state reduction of the *bc*₁ complexes with menadiol indicates that quinol is not oxidized through center P but is oxidized through center N. In addition, the levels of stigmatellin and UHDBT binding are markedly diminished, while antimycin binding is unaffected, in the *bc*₁ complexes with Rieske proteins lacking the disulfide bridge. Taken together, these results indicate that the ubiquinol oxidation site at center P is damaged in the *bc*₁ complexes with Rieske proteins lacking the disulfide bridge even though the iron–sulfur cluster is assembled into the Rieske protein.

The Rieske iron–sulfur protein is the redox protein with the highest midpoint potential in the cytochrome *bc*₁ complex. The high midpoint potential of the Rieske iron–sulfur cluster is the property that distinguishes it from other two-Fe-type iron–sulfur proteins (ferredoxins). Whereas the midpoint potentials of the Rieske centers range from 150 mV in menaquinol oxidizing organisms to 300 mV in ubiquinol oxidizing organisms (1, 2), the values for standard two-Fe ferredoxins range from –250 to –450 mV (3).

Part of the 400–750 mV potential difference between the Rieske proteins and the low-potential ferredoxins can be attributed to two histidine ligands to the redox active iron in the Rieske protein, as opposed to cysteines in the low-potential ferredoxins. However, the histidine ligands may account for only 100–300 mV of the difference, since biphenyl dioxygenase ferredoxin has a similar histidine ligation and a midpoint potential of approximately –150 mV (4). Additional contributions to the high midpoint potential

of the Rieske protein would be expected from the extensive hydrogen bonding network surrounding its iron–sulfur cluster, which is the major difference between the Rieske cluster and the dioxygenase iron–sulfur cluster. This was confirmed by site-directed mutagenesis of the yeast Rieske protein, in which it was shown that two hydrogen bonds into the cluster environment contributed as much as 175 mV to the high potential of the cluster (5). The potential increasing effect of the hydrogen bonds was confirmed by similar studies in the Rieske proteins of *Paracoccus denitrificans* (6) and *Rhodobacter sphaeroides* (7).

The [2Fe-2S] cluster of the Rieske iron–sulfur protein is held between two loops of the protein that are connected by a disulfide bridge as shown in Figure 1. The disulfide bridge is within van der Waals distance of the iron–sulfur cluster (Figure 1B) and thus might be expected to communicate electronically with the cluster. In addition, Zu and co-workers (2) showed that when the disulfide bridge in the Rieske protein of *Thermus thermophilus* was chemically reduced, reoxidation of the dithiol and the [2Fe-2S] cluster occurred rapidly and at the same potential. These results and a structural comparison of the cluster binding domain in the various classes of Rieske-type proteins (4) suggest that the

[†] This work was supported by NIH Grant GM 20379.

^{*} To whom correspondence should be addressed. Phone: (603) 650-1621. Fax: (603) 650-1128. E-mail: Trumpower@Dartmouth.edu.

[‡] Dartmouth Medical School.

[§] Universitätsklinikum Frankfurt.

^{||} Johann Wolfgang Goethe-Universität.

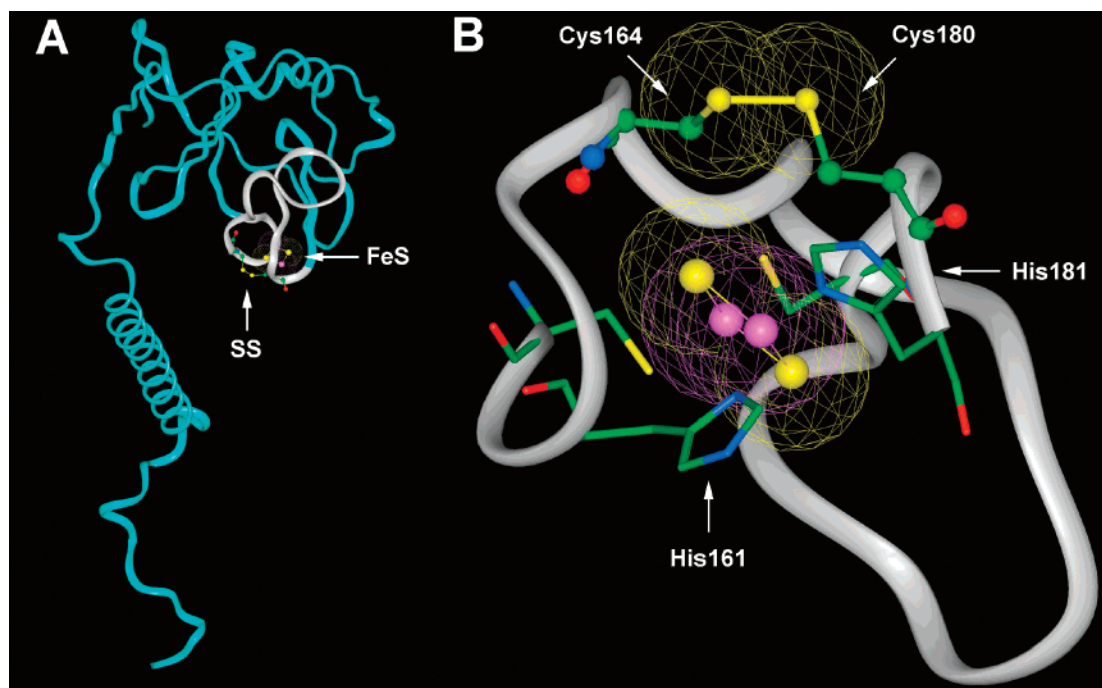


FIGURE 1: Structure of the Rieske iron-sulfur protein showing the disulfide bridge and the [2Fe-2S] cluster. Panel A shows a ribbon diagram of the Rieske iron-sulfur protein, excerpted from the crystal structure of the yeast cytochrome *bc*₁ complex [PDB entry 1EZV (23)]. The iron-sulfur cluster, with iron atoms colored magenta and sulfur atoms colored yellow, is ligated between two loops, β 4- β 5 and β 6- β 7. The van der Waals radii associated with the cluster are depicted as dots. The segment of the protein from Cys-159 through His-181 is colored gray. Cys-164 and Cys-180, which form the disulfide bridge between the two loops, are shown in ball-and-stick representation, with oxygen atoms colored red, carbon atoms colored green, nitrogen atoms colored blue, and sulfur atoms colored yellow. The transmembrane α -helix that anchors the iron-sulfur protein in the *bc*₁ complex is to the left of the globular domain that contains the iron-sulfur cluster. Panel B shows an expanded view of the segment of the protein from Cys-159 through His-181. The disulfide bridge formed by Cys-164 and Cys-180 and the iron-sulfur cluster are shown in ball-and-stick representation and colored as in panel A. The van der Waals radii of the sulfur atoms of the disulfide bridge and the iron-sulfur cluster are shown as a wire mesh surrounding the atoms. His-161 and His-181, ligands to the redox active iron, are shown in stick representation. The view in panel B is rotated relative to that in panel A so that the disulfide bridge is at the top.

disulfide bridge should affect the midpoint potential of the iron-sulfur cluster. Whether the disulfide bridge would contribute to the increase in the midpoint potential or lower it due to electron density from the sulfurs interacting with the orbitals surrounding the iron-sulfur cluster is not clear.

One would expect that the disulfide bridge may also stabilize the cluster binding domain. However, the iron-sulfur cluster of the Rieske-like ferredoxin of benzene dioxygenase and the irons of various rubredoxins are held between two loops that are structurally similar to those in the Rieske iron-sulfur protein but which lack the disulfide bridge (1). This suggests that the disulfide bridge may not be essential to the structural stability of the "Rieske-type" fold that is common to these iron-sulfur centers.

We thus sought to replace the cysteines that form the disulfide bridge by site-directed mutagenesis to evaluate the effect of the disulfide bridge on assembly, stability, and thermodynamic properties of the Rieske iron-sulfur cluster. In previous studies, various single-amino acid substitutions for either of the cysteines forming the disulfide bridge in *Saccharomyces cerevisiae* (8), *Rhodobacter capsulatus* (9), and *Rh. sphaeroides* (10) resulted in nonfunctional proteins. As noted above, the rubredoxins have a stable Rieske-type fold in which van der Waals interactions replace the disulfide bridge that is present in the Rieske protein. We thus reasoned that it might be possible to replace the cysteine residues in the yeast Rieske protein with pairs of non-sulfur-containing

amino acids, using the structures of the rubredoxins to inform the choice of alternative amino acids.

We have applied this rationale and successfully replaced Cys-164 and Cys-180 in the *S. cerevisiae* Rieske iron-sulfur protein with tyrosine and leucine, and tyrosine and valine. Here we describe the properties of the Rieske protein and the cytochrome *bc*₁ complexes isolated from these mutants.

EXPERIMENTAL PROCEDURES

Materials. Yeast nitrogen base (YNB)¹ without amino acids and with ammonium sulfate was from U.S. Biological. Amino acids were from Aldrich, Sigma, Fluka, and ICN. Dodecyl maltoside was obtained from Roche Molecular Biochemicals. DEAE-Biogel A was obtained from Bio-Rad Laboratories. Antimycin, diisopropyl fluorophosphate, phenylmethanesulfonyl fluoride, menadione, decylubiquinone, horse heart cytochrome *c*, and dithionite were purchased from Sigma Chemical Co. Stigmatellin was purchased from Fluka Biochemica. UHDBT was synthesized in our laboratory.

Purification of Cytochrome *bc*₁ Complexes. The yeast strains containing the mutations that eliminate the disulfide bridge of the Rieske protein are uracil-auxotrophic complements of Rieske deletion strain JPJ1 (11). The complemented

¹ Abbreviations: UHDBT, 3-undecyl-2-hydroxydioxobenzothiazol; YNB, yeast nitrogen base; DFP, diisopropyl fluorophosphate; NHE, normal hydrogen electrode; CD, circular dichroism.

strains carry the multicopy plasmids YEP352dR::RIP1, encoding the "wild-type" iron-sulfur protein; pJN192, encoding the Rieske iron-sulfur protein with C164Y and C180V mutations; and pJN182, encoding the Rieske iron-sulfur protein with C164Y and C180L mutations.

The strains were grown in 20 L carboys at room temperature on synthetic dropout medium containing 0.7% YNB, 0.14% amino acid mix lacking uracil, and 2% dextrose with aeration. Cells were harvested by centrifugation and broken in a Waring Blender in liquid nitrogen (12).

The cytochrome bc_1 complexes were extracted from mitochondrial membranes with dodecyl maltoside and purified by chromatography on DEAE-Biogel A as described previously (13, 14). The purified bc_1 complexes were concentrated by centrifugal filtration, using Amicon Centriprep YM-30 filtration units.

Western Blots. Mitochondrial membranes were extracted with dodecyl maltoside as described previously (13) with 1 mM DFP added to the extraction buffer immediately before extraction to protect the iron-sulfur protein from proteolysis. The extracts were bound to DEAE-Biogel A using a batch method, after which the resin was washed with 50 mM Tris-HCl, 1 mM $MgSO_4$, and 0.01% dodecyl maltoside (pH 7.4) containing 150 mM NaCl, and the bc_1 complexes were eluted with the same buffer containing 300 mM NaCl. The membranes and the bc_1 complexes were analyzed by Western blotting using antibodies against cytochrome c_1 and the Rieske iron-sulfur protein (15).

Absorption Spectroscopy. Optical absorption spectra of the bc_1 complexes were obtained with an Aminco DW2a UV-visible spectrophotometer with the OLIS DW2 conversion and OLIS software. The cytochrome c_1 concentration was determined from the difference spectrum of the ascorbate-reduced minus ferricyanide-oxidized enzyme, using an extinction coefficient of $17.5 \text{ mM}^{-1} \text{ cm}^{-1}$ at 553–540 nm. The cytochrome b concentration was determined from the difference spectrum of the dithionite-reduced minus ferricyanide-oxidized enzyme, using an extinction coefficient of $25 \text{ mM}^{-1} \text{ cm}^{-1}$ at 563–578 nm.

To measure the antimycin-induced red shift in the spectrum, the bc_1 complex was suspended at $3 \mu\text{M}$. A difference spectrum of the fully reduced enzyme with antimycin added versus the fully reduced enzyme was then recorded.

EPR Spectroscopy. EPR spectra were recorded at 20 K, a microwave frequency of 9.47 GHz, a microwave power of 1 mW, and a modulation amplitude of 0.64 mT using a Bruker ESP 300E spectrometer equipped with a liquid helium continuous flow cryostat, ESR 900, from Oxford Instruments. The bc_1 complex was diluted to approximately $30 \mu\text{M}$ in a buffer containing 250 mM sucrose, 50 mM potassium phosphate, 1 mM sodium azide, 0.2 mM EDTA, and 0.01% Tween 20 (pH 7.0). The samples were reduced with 5 mM ascorbate. As a control, the g_y signal intensity of the Rieske protein was compared to the signal intensity of the dithionite-reduced protein and found to be identical. After reduction, 3 equiv of UHDBT or stigmatellin was added when indicated and the samples were incubated for 20 min on ice. For baseline correction, a sample of the bc_1 complex without any addition, representing the oxidized state, was subtracted from the spectra of ascorbate-reduced samples.

Determination of the Midpoint Potentials of the Rieske Iron-Sulfur Centers. Midpoint potentials of the Rieske iron-

sulfur centers were determined by potentiometric titrations, and the redox status of the Rieske center was monitored by EPR spectroscopy. The bc_1 complexes were isolated as described above and concentrated by ultrafiltration to at least $30 \mu\text{M}$. Prior to the titrations, redox mediators were added to a final concentration of $33 \mu\text{M}$ of each to facilitate the redox equilibration of the enzyme. The mediators were chosen to cover the complete potential range from fully reduced to fully oxidized Rieske centers. The mediators and their midpoint potentials relative to NHE were menadione (-7 mV), duroquinone (7 mV), methylene blue (11 mV), phenazine methosulfate (80 mV), 1,2-naphthoquinone (145 mV), TMPD (260 mV), and ferrocyanide (408 mV). The EPR signals of these mediators do not overlap with the g_y signal of the Rieske iron-sulfur center, which was used to quantify the fraction of the reduced iron-sulfur cluster.

The bc_1 complexes with mediators were kept in an argon atmosphere at 25°C in 50 mM Tris, 1 mM $MgSO_4$, 0.01% dodecyl maltoside, and 300 mM NaCl (pH 7.4). Samples were taken under argon and immediately frozen after potential equilibration, which was controlled by a combination redox electrode. The complexes were first completely oxidized with ferrocyanide and then incrementally reduced with freshly prepared dithionite solutions in preparation buffer. The settings on the EPR spectrometer for the titrations were a temperature of 20 K, a microwave frequency of 9.47 GHz, a microwave power of 3.17 mW, and a modulation amplitude of 0.64 mT. The reduction status of the Rieske centers was determined by the relative intensities of the g_y signal in the EPR spectra and plotted versus applied potential.

Ubiquinol-Cytochrome c Reductase Assays. Ubiquinol-cytochrome c reductase activities of the purified bc_1 complexes were measured at room temperature in an assay buffer containing 50 mM potassium phosphate (pH 7.0), 250 mM sucrose, 1 mM sodium azide, 0.2 mM EDTA, 0.01% Tween 20, 0.5 mM potassium cyanide, and $50 \mu\text{M}$ cytochrome c . The cytochrome bc_1 complex from the wild-type yeast was added to a concentration of 2.5 nM, and the enzymes from the mutants were added to a concentration of 100 nM. The reaction was started by adding $50 \mu\text{M}$ decylubiquinol. Reduction of cytochrome c was monitored at 550–539 nm with the Aminco DW2a spectrophotometer in the dual-wavelength mode. An extinction coefficient of $21.5 \text{ mM}^{-1} \text{ cm}^{-1}$ at 550–539 nm was used to calculate the degree of cytochrome c reduction (16).

Pre-Steady-State Reduction of the bc_1 Complexes. Pre-steady-state reduction of the bc_1 complex was followed at room temperature by stopped-flow rapid scanning spectroscopy using the OLIS Rapid Scanning Monochromator (On-Line Instrument Systems, Inc., Bogart, GA) equipped with a 1200 lines/mm grating blazed at 500 nm. This produced a spectrum with a width of 75 nm, centered at 555 nm, with a resolution of 0.4 nm. Reactions were started by mixing $2 \mu\text{M}$ bc_1 complex in 50 mM potassium phosphate (pH 6.0), 250 mM sucrose, 1 mM sodium azide, 0.2 mM EDTA, and 0.01% Tween 20 against an equal volume of the same buffer containing $100 \mu\text{M}$ menadiol. A fresh solution of menadiol was prepared shortly before each experiment as described previously (14). The dead time of the instrument was $\sim 2 \text{ ms}$, and the end of this period was chosen as time zero. Data were collected at 1000 scans/s. A spectrum of the oxidized enzyme was subtracted from each averaged scan. From the

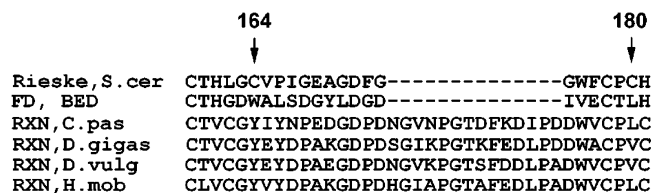


FIGURE 2: Amino acid sequences in the region surrounding the cysteine residues that form the disulfide bridge in the Rieske iron-sulfur protein and in homologous regions of Rieske-type proteins. The top sequence is from Cys-159 to His-181 in the Rieske protein from *S. cerevisiae*. Below that are sequences in structurally homologous regions of the benzene dioxygenase ferredoxin from *Pseudomonas putida* and the rubredoxins from *Clostridium pasteurianum*, *Desulfovibrio gigas*, *Desulfovibrio vulgaris*, and *Helicobacter mobilis*.

three-dimensional data set comprised of wavelength, absorbance, and time, the time course and amplitude change for cytochrome *b* reduction at 563 nm and cytochrome *c*₁ reduction at 553 nm were extracted using the OLIS software.

RESULTS

Replacement of the Cysteine Residues Forming the Disulfide Bridge. Various iron-sulfur proteins, including the [2Fe-2S] benzene dioxygenase ferredoxin and numerous single-Fe center rubredoxins, contain a Rieske-type cluster domain. This was first pointed out when it was noted that the cluster binding fold of the bovine Rieske iron-sulfur protein could be superimposed on the cluster binding fold of various rubredoxins (17). However, these mononuclear iron proteins lack the covalent disulfide bridge that is present in the Rieske iron-sulfur protein and contain instead pairs of amino acids capable of aliphatic-aliphatic or aromatic-aliphatic van der Waals interactions. This suggests that the disulfide bridge in the Rieske iron-sulfur protein might be dispensable, if replaced by appropriate pairs of amino acids that could mimic the interactions found in the dioxygenase ferredoxin or the rubredoxins.

The sequence of amino acids surrounding the disulfide bridge in the yeast Rieske protein and the sequences in the structurally homologous regions of a benzene dioxygenase and several rubredoxins are aligned for comparison in Figure 2. There is only a low degree of sequence identity between this region of the Rieske protein and the other five iron-sulfur proteins, and the rubredoxins contain a 14-amino acid insert that extends one of the cluster binding loops in those proteins. The dioxygenase sequence is only 26% identical to the yeast sequence, and the sequences of the rubredoxins, excluding the inserted amino acids, are only 35–40% identical to the yeast sequence. However, with crystal structures to guide the alignment, it is possible to determine that a Trp/Leu pair in the dioxygenase occurs at a position occupied by the two cysteines in the Rieske protein. In the rubredoxins, a tyrosine occupies the position equivalent to Cys-164 and leucine or valine occupies the position equivalent to Cys-180 in the Rieske protein.

With these structures as a guide, we replaced Cys-164 and Cys-180 in the yeast Rieske protein by site-directed mutagenesis to create C164Y/C180L, C164Y/C180V, C164W/C180L, and C164W/C180A double mutations. We also created a C164S/C180S double mutation because of the structural similarity between serine and cysteine. We introduced these mutations on the RIP1 gene encoding the iron-

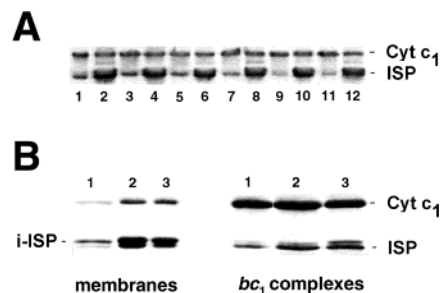


FIGURE 3: Western blots of mitochondrial membranes and isolated cytochrome *bc*₁ complexes from yeast strains expressing Rieske proteins that lack the disulfide bridge. Panel A shows the blot of mitochondrial membranes from yeast strains containing mutations that eliminate the disulfide bridge and from the complemented wild-type strain. The membrane samples are from the complemented wild-type strain (lanes 1 and 2) and mutants C164Y/C180L (lanes 3 and 4), C164Y/C180V (lanes 5 and 6), C164W/C180L (lanes 7 and 8), C164W/C180A (lanes 9 and 10), and C164S/C180S (lanes 11 and 12). Lanes 1, 3, 5, 7, 9, and 11 show membranes from yeast strains carrying the RIP1 gene or mutated RIP1 gene on a single-copy plasmid, and lanes 2, 4, 6, 8, 10, and 12 show membranes from yeast strains with the RIP1 genes on multi-copy plasmids. In panel B, the three lanes at the left contain mitochondrial membranes and the three lanes at the right contain purified *bc*₁ complexes from the wild-type yeast (lane 1), the C164Y/C180L mutant (lane 2), and the C164Y/C180V mutant (lane 3). The blots were probed with monoclonal antibodies to cytochrome *c*₁ and the Rieske protein. The migration positions of cytochrome *c*₁ (Cyt *c*₁), the intermediate iron-sulfur protein (i-ISP), and the mature iron-sulfur protein (ISP) are marked.

sulfur protein into single-copy and high-copy number plasmids. We then transformed these plasmids into a yeast strain, JPJ1, in which the chromosomal copy of the RIP1 gene is deleted (11) to create yeast strains carrying the double mutations in the Rieske iron-sulfur protein gene.

We previously showed that mutations that prevent insertion of the iron-sulfur cluster result in decreased amounts of the Rieske protein in the mitochondrial membranes, presumably because of the instability of the protein (18). To identify yeast mutants that express the Rieske protein at a concentration comparable to that of the wild-type strain, we performed Western blot analysis on mitochondrial membranes of the mutants carrying single-copy and multi-copy plasmids using the rationale that higher levels of protein derived from the latter might compensate for protein instability. The concentration of the Rieske protein relative to cytochrome *c*₁ was used as an indicator of the protein's stability. As seen in Figure 3A, only two of the mutants, C164Y/C180L (lane 3) and C164Y/C180V (lane 5), contain Rieske protein at a level similar to that of the wild-type yeast (lane 1) when the genes are expressed from single-copy plasmids. Consequently, we chose the C164Y/C180L and C164Y/C180V mutants for further characterization. These mutations recapitulate the pairs of amino acids occurring in the rubredoxins (Figure 2) and thus seemed likely to confer sufficient stability on the Rieske protein to allow purification and characterization of the *bc*₁ complexes containing the mutant proteins.

Further Western blot analysis (Figure 3B) of membranes from the yeast with the C164Y/C180L and C164Y/C180V double mutations and the wild-type yeast and of the *bc*₁ complexes isolated from these membranes showed that the ratio of Rieske protein to cytochrome *c*₁ in the mutants (lanes 2 and 3) was as high as in the strain complemented with the RIP1 gene from wild-type yeast (lane 1). These blots also

showed that significant amounts of i-ISP accumulated in the membranes when the gene was expressed from a multi-copy plasmid and that some i-ISP was integrated into the bc_1 complexes, as evidenced by its presence in the isolated enzymes. The latter observation is consistent with our previous finding that the intermediate-sized iron–sulfur protein is present and functionally active in the yeast bc_1 complex (19).

Properties of the Cytochrome bc_1 Complexes Containing Mutated Rieske Iron–Sulfur Proteins. Optical spectra of the isolated bc_1 complexes of the two disulfide mutants showed no significant difference compared to the spectrum of the enzyme from wild-type yeast, judged from spectra of the fully reduced minus oxidized enzymes (results not shown). Difference spectra indicated a 2:1 ratio of cytochrome b to cytochrome c_1 in the mutants and the wild-type enzyme (not shown). The spectra thus establish that these mutations of the disulfide bridge in the Rieske protein do not impair the stability of the cytochromes. This contrasts with the marked decrease in the cytochrome b optical spectrum that results from deletion of the iron–sulfur protein gene (20).

Antimycin binds to cytochrome b at the Q_N site of the bc_1 complex and induces a bathochromic shift in the absorption maximum of reduced cytochrome b (21). Difference spectra of the reduced enzyme with and without antimycin bound showed that antimycin binds to cytochrome b of the mutants and causes a shift in the optical spectrum similar to that induced in the spectrum of the bc_1 complex from wild-type yeast (results not shown).

CD spectroscopy and X-band EPR spectroscopy of the bc_1 complexes indicated that the [2Fe-2S] iron–sulfur cluster is assembled in the bc_1 complexes of the disulfide mutants. The CD spectra of the reduced bc_1 complexes (results not shown) showed a negative signal centered around 500 nm which is typical for all Rieske proteins (22). However, the EPR spectra of the reduced bc_1 complexes showed strongly altered features of the [2Fe-2S] iron–sulfur cluster (Figure 4). EPR spectra taken at higher enzyme concentrations in the absence of the inhibitory ligands allowed assignment of the g_x signals, which were not visible in the spectra shown in Figure 4. From the former spectra, we calculated the extent of rhombicity in the spectra of the disulfide mutants (Table 1). Both mutants exhibited more rhombic EPR spectra with shifted g values compared to the spectrum of the wild-type Rieske protein.

Stigmatellin and UHDBT bind to the Q_P center of the bc_1 complex, and both inhibitors interact with the Rieske iron–sulfur protein through a hydrogen bond to the imidazole nitrogen of a histidine that is a ligand to the [2Fe-2S] iron–sulfur cluster (23, 24). This interaction shifts all three signals in the EPR spectrum of the Rieske protein from the wild-type yeast, having the most noticeable effects on the g_x and g_y signals. Stigmatellin, which binds more tightly than UHDBT, has the more pronounced effect on the EPR spectrum, shifting the g_x and g_y signals in the spectrum to 1.78 and 1.889, respectively, while UHDBT shifts these signals to 1.77 and 1.888, respectively, as shown in Figure 4A. These ligands have little, if any, effect on the EPR spectra of the Rieske proteins from the disulfide bond mutants. The spectrum of the bc_1 complex of the C164Y/C180L mutant shows a slight sharpening and a shift of the g_x signal to 1.78, in the presence of stigmatellin (Figure 4B),

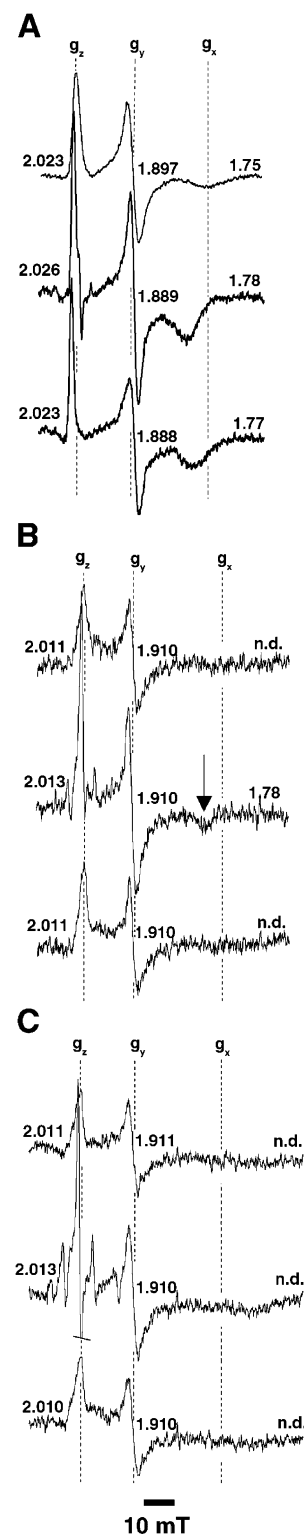


FIGURE 4: EPR spectra of cytochrome bc_1 complexes from yeast mutants lacking the disulfide bridge in the Rieske iron–sulfur protein, showing the effects of stigmatellin and UHDBT. The spectra in panel A are of the bc_1 complex from the wild-type yeast; those in panel B are from the C164Y/C180L mutant, and those in panel C are from the C164Y/C180V mutant. In the three sets of spectra, the top spectrum was obtained in the absence of added ligand, the middle spectrum in the presence of stigmatellin, and the bottom spectrum in the presence of UHDBT. The arrow in panel B points to the g_x resonance in the spectrum from the C164Y/C180L mutant in the presence of stigmatellin. The dashed lines are drawn through the indicated resonance peaks in the control spectrum without any inhibitor to emphasize the shifts of the g_x , g_y , and g_z signals as a result of inhibitor binding.

Table 1: EPR Spectral Parameters of the [2Fe-2S] Rieske Cluster in Wild-Type Yeast and Yeast Mutants Lacking the Disulfide Bridge in the Rieske Protein^a

yeast strain	g_z	g_y	g_x	g_{av}	R_z
wild-type	2.025	1.897	1.76	1.895	106%
C164Y/C180L	2.013	1.908	1.70	1.877	149%
C164Y/C180V	2.013	1.908	1.72	1.883	142%

^a Rhombicity (R_z) = $300(g_y - g_x)/(2g_z - g_y - g_x)$. If the rhombicity is 100%, the EPR spectrum has no preferential axis. If the value deviates from 100%, as is the case for both of the mutants, the spectra are more axial.

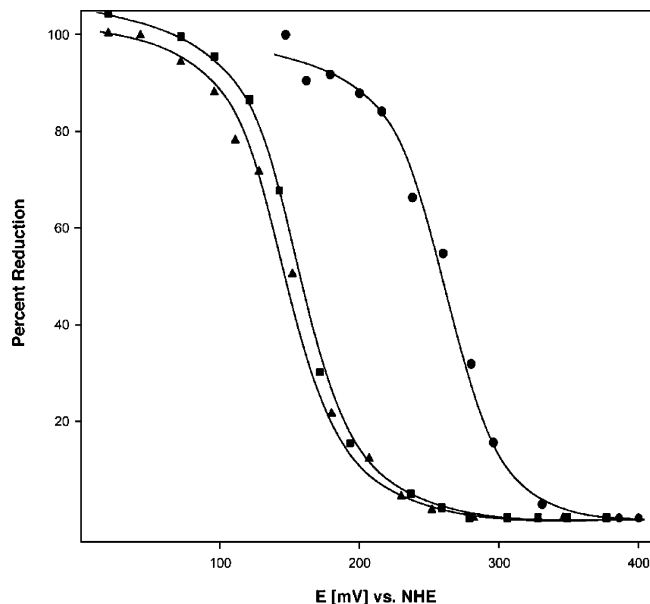


FIGURE 5: Potentiometric titrations of the Rieske iron-sulfur center in bc_1 complexes with Rieske proteins lacking the disulfide bridge. Potentiometric titrations were performed at pH 7.4. The data for the titration for the bc_1 complex from the wild-type yeast are represented with solid circles. The data for the titration for the bc_1 complex from the C164Y/C180L mutant are represented with solid triangles, and those for the bc_1 complex from the C164Y/C180V mutant are represented with solid squares. The solid lines are fits to $n = 1$ Nernstian curves.

and the g_z signals in both mutants (Figure 4B,C) shifted slightly from 2.011 to 2.013 upon addition of stigmatellin. However, these changes are small compared to the effects of stigmatellin on the spectrum of the enzyme from wild-type yeast (Figure 4A). There was no effect of UHDBT on the EPR spectrum of either of the mutants (Figure 4B,C). Together, these results indicate that binding of ligands at the Q_P center is impaired in both of these disulfide bond mutants.

To determine how the midpoint potentials of the Rieske iron-sulfur centers are affected by the replacement of the disulfide bridge, we performed redox titrations on the purified bc_1 complexes and monitored the redox status of the Rieske center by EPR spectroscopy (Figure 5). The midpoint potentials of the [2Fe-2S] centers of the mutants were shifted by -115 and -105 mV, from 265 mV in the Rieske protein from wild-type yeast to 150 mV in the protein from the C164Y/C180L mutant and to 160 mV in the protein from the C164Y/C180V mutant, respectively. These changes in midpoint potential are the opposite of what we expected, since removal of the electron-donating sulfurs would remove electron density from the [2Fe-2S] center, which would raise

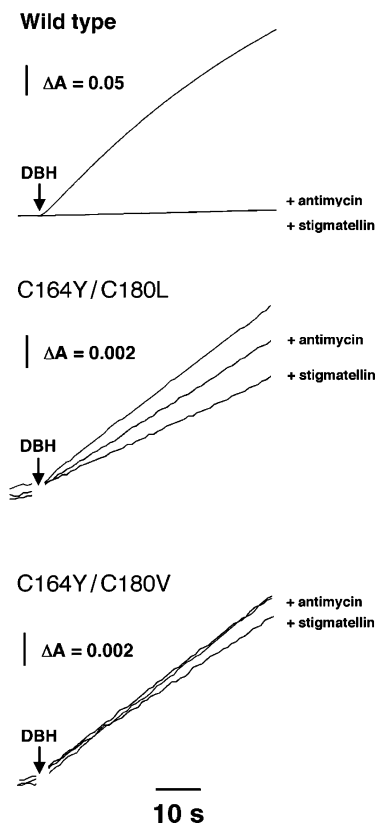


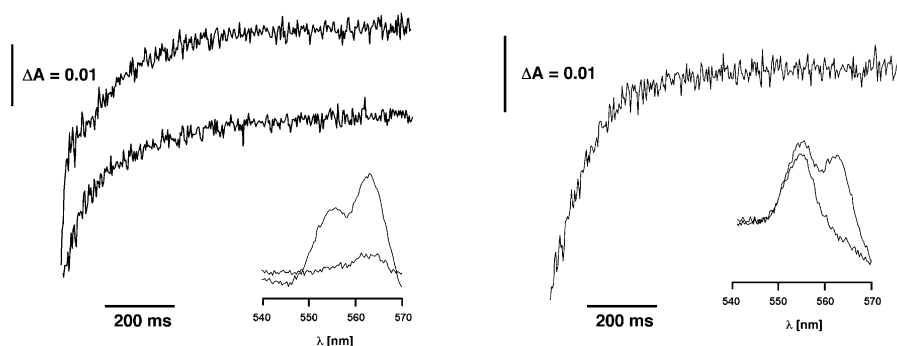
FIGURE 6: Ubiquinol-cytochrome c reductase activities of cytochrome bc_1 complexes with Rieske proteins lacking the disulfide bridge. The activity of the bc_1 complex from the wild-type yeast was measured with 2.5 nM enzyme in the assays, while the activities of the enzymes from the mutants were measured with 100 nM enzyme in the assays. Note that the absorbance scales are also different in the assays for the mutant and wild-type enzymes. The enzymes were preincubated with 3 equiv of antimycin or stigmatellin prior to initiation of the assay with decylubiquinol, where indicated.

the midpoint potential of the cluster. The basis for the change in midpoint potentials is discussed below.

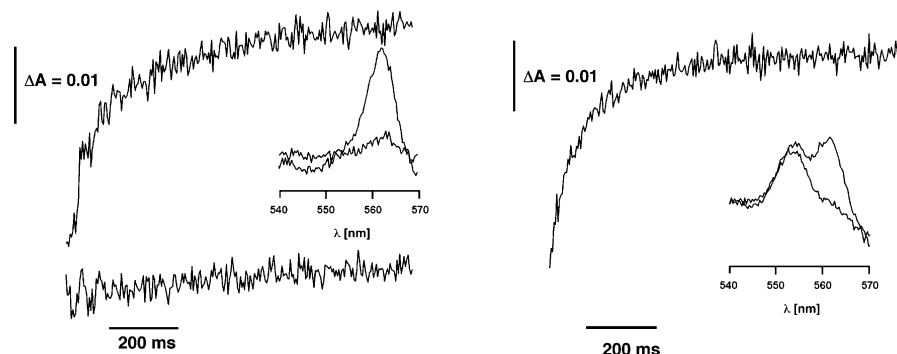
Ubiquinol-cytochrome c reductase activities of the disulfide bridge mutants were decreased, as shown in Figure 6, from 135 s^{-1} in the wild-type enzyme to 0.06 s^{-1} in the mutants. These activities are much lower than would be expected solely on the basis of the lowered midpoint potential of the Rieske protein. When the midpoint of the Rieske iron-sulfur cluster was reduced to 155 mV by an S183A mutation in the protein, the activity of that bc_1 complex was 10% of that of the wild-type enzyme (5). This comparison suggests that the disulfide bond mutations have introduced secondary structural changes into the ubiquinol oxidation site at center P, beyond any effects on the electronic environment surrounding the iron-sulfur cluster.

Further evidence for structural changes at the Q_P center can be seen in the incomplete inhibition of the ubiquinol-cytochrome c reductase activities of the bc_1 complexes from the disulfide bridge mutants by stigmatellin and antimycin (Figure 6). Whereas both of these inhibitors reduced the activity of the bc_1 complex from wild-type yeast by more than 95%, stigmatellin inhibited the bc_1 complex from the C164Y/C180L mutant by only 60% and antimycin inhibited it by only 30%. The inhibitors were even less effective on the enzyme from the C164Y/C180V mutant, in which case stigmatellin and antimycin inhibited the complex by only

Wild type



C164Y / C180L



C164Y / C180V

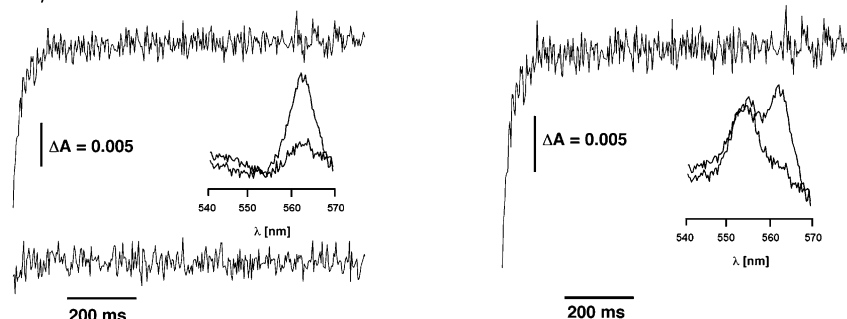


FIGURE 7: Pre-steady-state reduction of cytochrome bc_1 complexes from wild-type yeast and mutants lacking the disulfide bridge in the Rieske iron–sulfur protein. The traces on the left show reduction of the bc_1 complexes by 50 μ M menadiol, and the traces on the right show reduction of the bc_1 complexes by 50 μ M menadiol after prereduction of cytochrome c_1 by ascorbate. The insets show optical spectra before and after the reduction with menadiol.

30 and 5%, respectively. How damage to the Q_P center could compromise inhibition by both stigmatellin and antimycin is discussed below.

To confirm that the loss of ubiquinol–cytochrome c reductase activity was due to an impaired Q_P center, we examined the pre-steady-state reduction of the bc_1 complexes by menadiol. As can be seen in Figure 7, menadiol rapidly reduces both cytochromes b and c_1 in the bc_1 complex from wild-type yeast but reduces only cytochrome b in the enzymes from the disulfide bridge mutants. If reduction of cytochrome b through the Q_P center is blocked by prior reduction of cytochrome c_1 by ascorbate, menadiol can reduce cytochrome b through the Q_N center. This reduction occurs in both mutant and wild-type enzymes, confirming that the Q_N center is functional in the mutants. Reduction of cytochrome b through the Q_N center was inhibited by

antimycin in both the mutant and wild-type enzymes (results not shown).

DISCUSSION

Our results demonstrate that the [2Fe-2S] cluster of the Rieske iron–sulfur protein can be assembled if the disulfide bridge that connects the two loops of the protein surrounding the cluster is replaced with amino acids capable of making van der Waals interactions. Eliminating the disulfide bridge also did not significantly impair the stability of the cluster, which remained intact during the approximately 3 h period at room temperature required to perform the potentiometric titrations. However, eliminating the disulfide bridge resulted in significant structural changes in the Rieske protein environment around the [2Fe-2S] cluster. These structural changes in turn affect the interaction of the cluster-bearing

domain of the Rieske protein with ubiquinol at the Q_P site and thus indirectly damage the ubiquinol oxidation site.

From the crystal structures of the iron–sulfur protein (17, 23), we expected that the soft electron shell of the disulfide bridge would contribute electron density to the iron–sulfur center. If so, eliminating the disulfide bridge should raise the midpoint potential of the iron–sulfur center. However, we found the opposite effect, in that the midpoint potentials of the C164Y/C180V and C164Y/C180L mutants were decreased by 105–115 mV. This result agrees with the previous findings of Zu and co-workers (2), who showed that reduction and irreversible bisalkylation of the disulfide bridge lowered the low-pH midpoint potential of the Rieske protein by approximately 125 mV. Similarly, Davidson and co-workers found that mutations that eliminate the disulfide bridge in the Rieske protein of *Rh. capsulatus* lower the midpoint potential by approximately 180 mV (9).

One explanation for our results and others (2, 9) is that lowering of the midpoint potentials by elimination of the disulfide bridge occurs because the sulfurs delocalize electron density out of rather than donate electron density into the cluster environment. The decline in midpoint potential may also be partly due to the loss of hydrogen bond interactions. Zu and co-workers (2) noted that the loss of the disulfide bond which tethers the ligand-bearing loops of the Rieske protein correlates with a lack of H-bond interactions in the low-potential benzene dioxygenase from *Burkholderia* sp. strain LB400. And finally, lowering of the midpoint potentials by the mutations may also reflect a more complex structural change in the cluster environment.

Structural alterations in the iron–sulfur cluster were revealed by the EPR spectra. In an early work on interpretation of EPR spectra of the binuclear iron–sulfur protein, Blumberg and Peisach noted the unusually low g_{av} value of the Rieske cluster (25). Although the g values in the spectra of the two mutants fall in the range of known Rieske or Rieske-type [2Fe-2S] iron–sulfur centers, the g_{av} values are among the lowest and the degree of rhombicity is among the highest observed so far. The g_{av} value of 1.877 for the C164Y/C180L mutant appears to be the lowest value observed for any Rieske or Rieske-type protein.

The bc_1 complexes with Rieske iron–sulfur proteins lacking the disulfide bridge almost completely lacked ubiquinol-cytochrome *c* reductase activity. This could not be explained by the decrease in the midpoint potential of the Rieske centers in these mutants, because other mutants in which the midpoint potential of the Rieske center is decreased to 150 mV exhibit as much as 10% of the wild-type activity (5, 6). Pre-steady-state reduction of the bc_1 complexes from the mutants showed that cytochrome *b* could be reduced through the Q_N center but that cytochrome c_1 could not be reduced through the Q_P center except at an extremely slow rate (results not shown). This suggests that the ubiquinol oxidation site at center P is damaged as an indirect consequence of structural changes in the cluster-bearing domain resulting from elimination of the disulfide bridge. The damage to the quinol oxidation site appears not to be a change in specificity for the quinol substrate. The rate of oxidation of ubiquinol in the cytochrome *c* reductase assay and the pre-steady-state rate of cytochrome *b* and c_1 reduction through center P were affected to the same extent.

Structural damage to the ubiquinol oxidation site was also indicated by the lack of inhibition of the residual cytochrome *c* reductase activities of the mutants by stigmatellin. Altered stigmatellin and UHDBT binding was confirmed by the EPR spectra, which reveal the interaction of these ligands with the Rieske center. Since stigmatellin and UHDBT are considered to be structural mimetics of ubiquinol or ubisemiquinone, these changes are independent indications that ubiquinol binding at center P is impaired.

The lack of inhibition of the residual cytochrome *c* reductase activities of the mutants by antimycin is noteworthy, since this inhibitor blocks ubiquinone reduction through the Q_N center and this reaction was blocked in the mutants. In addition, optical spectra indicated that antimycin binds to cytochrome *b* at the Q_N site in the mutant bc_1 complexes. Oxidation of ubiquinol at center P is normally a bifurcated reaction in which one electron from ubiquinol is passed through the iron–sulfur protein to cytochrome c_1 while the other is passed to the *b* cytochromes, which then reduce ubiquinone. Inhibition of the latter reaction by antimycin blocks recycling of electrons through the *b* cytochromes and inhibits the Q cycle (26). The lack of antimycin inhibition suggests that the bifurcated oxidation is disrupted in these mutants such that electrons from ubiquinol are transferred to cytochrome c_1 but not to cytochrome *b*. This is similar to the “bypass reactions” at center P observed by Muller and co-workers (27), in which ubiquinol could access the Rieske center but not cytochrome *b* in the presence of inhibitors that bind proximal to the b_L heme.

ACKNOWLEDGMENT

We thank Prof. Dr. Ulrich Brandt (Frankfurt, Germany) for use of the EPR spectrometer and laboratory facilities.

REFERENCES

- Link, T. A. (1999) The structures of Rieske and Rieske-type proteins, *Adv. Inorg. Chem.* 47, 83–157.
- Zu, Y., Fee, J. A., and Hirst, J. (2002) Breaking and re-forming the disulfide bond at the high-potential, respiratory-type Rieske [2Fe-2S] center of *Thermus thermophilus*: Characterization of the sulfhydryl state by protein-film voltammetry, *Biochemistry* 41, 14054–14065.
- Beinert, H., Holm, R. H., and Münck, E. (1997) Iron–sulfur clusters: Nature’s modular, multipurpose structures, *Science* 277, 653–659.
- Colbert, C. L., Couture, M. M.-J., Eltis, L. D., and Bolin, J. T. (2000) A cluster exposed: Structure of the Rieske ferredoxin from biphenyl dioxygenase and the redox properties of Rieske Fe–S proteins, *Structure* 8, 1267–1278.
- Denke, E., Merbitz-Zahradnik, T., Hatzfeld, O. M., Snyder, C., Link, T. A., and Trumpower, B. L. (1998) Alteration of the midpoint potential and catalytic activity of the Rieske iron–sulfur protein by changes of amino acids forming hydrogen bonds to the iron–sulfur cluster, *J. Biol. Chem.* 273, 9085–9093.
- Schröter, T., Hatzfeld, O. M., Gemeinhardt, S., Korn, M., Friedrich, T., Ludwig, B., and Link, T. A. (1998) Mutational analysis of residues forming hydrogen bonds in the Rieske [2Fe-2S] cluster of the cytochrome bc_1 complex in *Paracoccus denitrificans*, *Eur. J. Biochem.* 255, 100–106.
- Guergova-Kuras, M., Kuras, R., Ugulava, N., Hadad, I., and Crofts, A. R. (2000) Specific mutagenesis of the Rieske iron–sulfur protein in *Rhodobacter sphaeroides* shows that both the thermodynamic gradient and the pK of the oxidized form determine the rate of quinol oxidation by the bc_1 complex, *Biochemistry* 39, 7436–7444.
- Graham, L. A., Brandt, U., Sargent, J. S., and Trumpower, B. L. (1993) Mutational analysis of assembly and function of the iron–

- sulfur protein of the cytochrome bc_1 complex in *Saccharomyces cerevisiae*, *J. Bioenerg. Biomembr.* 25, 245–257.
9. Davidson, E., Ohnishi, T., Atta-Asafo-Adeji, E., and Daldal, F. (1992) Potential ligands to the [2Fe-2S] Rieske cluster of the cytochrome bc_1 complex of *Rhodobacter capsulatus* probed by site-directed mutagenesis, *Biochemistry* 31, 3342–3351.
 10. Van Doren, S. R., Gennis, R. B., Barquera, B., and Crofts, A. R. (1993) Site-directed mutations of conserved residues of the Rieske iron–sulfur subunit of the cytochrome bc_1 complex of *Rhodobacter sphaeroides* blocking or impairing quinol oxidation, *Biochemistry* 32, 8083–8091.
 11. Beckmann, J. D., Ljungdahl, P. O., and Trumpower, B. L. (1989) Mutational analysis of the mitochondrial Rieske iron–sulfur protein of *Saccharomyces cerevisiae* I. Construction of a RIP1 deletion strain and isolation of temperature sensitive mutants, *J. Biol. Chem.* 264, 3713–3722.
 12. Snyder, C. H., Denke, E., and Trumpower, B. L. (1999) Aromatic amino acids in the Rieske iron–sulfur protein do not form an obligatory conduit for electron transfer from the iron–sulfur cluster to the heme of cytochrome c_1 in the cytochrome bc_1 complex, *Biochim. Biophys. Acta* 1410, 237–247.
 13. Ljungdahl, P. O., Pennoyer, J. D., Robertson, D., and Trumpower, B. L. (1987) Purification of highly active cytochrome bc_1 complexes from phylogenetically diverse species by a single chromatographic procedure, *Biochim. Biophys. Acta* 891, 227–242.
 14. Snyder, C., and Trumpower, B. L. (1998) Mechanism of ubiquinol oxidation by the cytochrome bc_1 complex: Presteady-state kinetics of cytochrome bc_1 complexes containing site-directed mutants of the Rieske iron–sulfur protein, *Biochim. Biophys. Acta* 1365, 125–134.
 15. Nett, J. H., and Trumpower, B. L. (1996) Dissociation of import of the Rieske iron–sulfur protein into *Saccharomyces cerevisiae* mitochondria from proteolytic processing of the presequence, *J. Biol. Chem.* 271, 26713–26716.
 16. Cavazzoni, M., Svobodova, J., Desantis, A., Fato, R., and Lenaz, G. (1993) Steady-state kinetics of ubiquinol cytochrome c reductase in *Saccharomyces cerevisiae* mitochondria: Effects of fluidity changes obtained by different growth temperatures, *Arch. Biochem. Biophys.* 303, 246–254.
 17. Iwata, W., Saynovits, M., Link, T. A., and Michel, H. (1996) Structure of a water soluble fragment of the ‘Rieske’ iron sulfur protein of the bovine heart mitochondrial cytochrome bc_1 complex determined by MAD phasing at 1.5 angstrom resolution, *Structure* 4, 567–579.
 18. Graham, L., and Trumpower, B. L. (1991) Mutational Analysis of the Mitochondrial Rieske Iron–Sulfur Protein of *Saccharomyces cerevisiae* III. Import, Protease Processing, and Assembly into the Cytochrome bc_1 Complex of Iron–Sulfur Protein Lacking the Iron–Sulfur Cluster, *J. Biol. Chem.* 266, 22485–22492.
 19. Nett, J., and Trumpower, B. L. (1999) Intermediate length Rieske iron–sulfur protein is present and functionally active in the cytochrome bc_1 complex of *Saccharomyces cerevisiae*, *J. Biol. Chem.* 274, 9253–9257.
 20. Ljungdahl, P. O., Beckmann, J. D., and Trumpower, B. L. (1989) Mutational analysis of the mitochondrial Rieske iron–sulfur protein of *Saccharomyces cerevisiae* II. Biochemical characterization of temperature sensitive rip 1[–] mutants, *J. Biol. Chem.* 264, 3723–3731.
 21. Slater, E. C. (1973) The mechanism of action of the respiratory inhibitor, antimycin, *Biochim. Biophys. Acta* 301, 129–154.
 22. Degli-Esposti, M., Ballester, F., Solaini, G., and Lenaz, G. (1987) The circular-dichroic properties of the Rieske iron–sulfur protein in the mitochondrial ubiquinol:cytochrome c reductase, *Biochem. J.* 241, 285–290.
 23. Hunte, C., Koepke, J., Lange, C., Rossmanith, T., and Michel, H. (2000) Structure at 2.3 angstrom resolution of the cytochrome bc_1 complex from the yeast *Saccharomyces cerevisiae* co-crystallized with an antibody Fv fragment, *Structure* 8, 669–684.
 24. Palsdottir, H., Gomez Lojero, C., Trumpower, B. L., and Hunte, C. (2003) Structure of the yeast cytochrome bc_1 complex with a hydroxyquinone anion Q_o site inhibitor bound, *J. Biol. Chem.* 278, 31303–31311.
 25. Blumberg, W. E., and Peisach, J. (1974) On the interpretation of electron paramagnetic resonance spectra of binuclear iron–sulfur proteins, *Arch. Biochem. Biophys.* 162, 502–512.
 26. Trumpower, B. L. (1990) The protonmotive Q cycle: Coupling of proton translocation to electron transfer by the cytochrome bc_1 complex, *J. Biol. Chem.* 265, 11409–11412.
 27. Muller, F., Crofts, A. R., and Kramer, D. M. (2002) Multiple Q-cycle bypass reactions at the $Q_{(O)}$ site of the cytochrome bc_1 complex, *Biochemistry* 41, 7866–7874.

BI035344R